

NASA Technical Memorandum 85693

NASA-TM-85693 19840009976

Neon Transport in Selected Organic Composites

LIBRARY COPY

LANGLEY RESEARCH CENTER
LIBRARY, NASA
HAMPSHIRE, NEW HAMPSHIRE

Lawrence W. Townsend, John W. Wilson,
and Hari B. Bidasaria

FEBRUARY 1984

FOR REFERENCE

NOT TO BE TAKEN FROM THIS ROOM

NASA

NASA Technical Memorandum 85693

Neon Transport in Selected Organic Composites

Lawrence W. Townsend and John W. Wilson
Langley Research Center
Hampton, Virginia

Hari B. Bidasaria
Old Dominion University
Norfolk, Virginia



National Aeronautics
and Space Administration

**Scientific and Technical
Information Office**

1984

Use of trade names or names of manufacturers in this report does not constitute an official endorsement of such products or manufacturers, either expressed or implied, by the National Aeronautics and Space Administration.

INTRODUCTION

As the era of the Space Transportation System progresses toward the possible development of a permanent manned presence in space, long-term exposure of astronauts and equipment to large fluences of galactic heavy ions indicates a need to investigate methods of shielding from these high-energy ions. To properly evaluate the passive shield requirements, a comprehensive theory describing the interaction and propagation of these particles, and their subsequent reaction products, in the spacecraft structure and in the inhabitants is required. The nuclear interaction model used is described in detail in references 1 and 2 (and references therein). The heavy-ion propagation is described by an energy-dependent extension of the transport theory given in reference 3. Polyethylene and Du Pont Kapton were chosen for the analyses since they may be used as constituents of a multilayered shield design to replace the usual bulk metallic spacecraft shielding. In the present report, transport coefficients for arbitrary ions incident upon Kapton and polyethylene absorbers are presented over a broad range of energies. The results of the transport theory are illustrated by calculating the doses from ^{20}Ne beams at 350, 670, and 2000 MeV/amu as a function of depth in the absorbers.

DEPTH-DOSE EXPRESSIONS

With the straight-ahead approximation and the target secondary fragments neglected, the transport equation is written as

$$\left[\frac{\partial}{\partial x} - \frac{\partial}{\partial E} \tilde{S}_j(E) + \sigma_j(E) \right] \phi_j(x, E) = \sum_{k>j} m_{jk}(E) \sigma_k(E) \phi_k(x, E) \quad (1)$$

where $\phi_j(x, E)$ is the flux of ions of type j with atomic mass A_j at x moving along the x -axis at energy E in units of MeV/amu, $\sigma_j(E)$ is the corresponding macroscopic nuclear absorption cross section, $\tilde{S}_j(E)$ is the specific stopping power (change in E per unit distance), and $m_{jk}(E)$ is the fragmentation parameter of ion j produced in collision by ion k . (A list of symbols appears after the references in this report.) In terms of the specific stopping power, the range of the ion is

$$R_j(E) = \int_0^E \frac{dE'}{\tilde{S}_j(E')} \quad (2)$$

Using an iterative procedure (ref. 3), equation (1) is solved by the method of characteristics. The resultant series solution is used to evaluate the dose as a function of depth as follows:

$$D(x) = \sum_j \int_0^\infty dE \tilde{S}_j(E) \phi_j(x, E) \quad (3)$$

for a monoenergetic beam on type-M ions of energy E_0 , where the stopping power is

$$S_j = A_j \tilde{S}_j \quad (4)$$

The dose from the radiation field of the primary (incident) beam, obtained by setting the right-hand side of equation (1) equal to zero, is given by

$$D^{(0)}(x) = \frac{S_M(E_x) P_M(E_0)}{P_M(E_x)} \quad (5)$$

where the nuclear attenuation factors are

$$P_M(E) = \exp[-O_M(E) R_M(E)] \quad (6)$$

The average extinction coefficient is defined as

$$O_M(E) = \left[\int_0^E \sigma_M(e) de / \tilde{S}_M(e) \right] / R_M(E) \quad (7)$$

and the residual energy is

$$E_x = R_M^{-1} [R_M(E_0) - x] \quad (8)$$

The first perturbation to the homogeneous solution yields the dose contribution from the secondary ions produced by the fragmentation of the primary beam. This contribution is

$$\begin{aligned} D^{(1)}(x) \approx \sum_j A_j v_j (E_{u_j} - E_{\ell_j}) & \left[\frac{m_{jM}(E_0) \sigma_M(E_0) P_j(E_0)}{P_j(E_{\ell_j})} \right. \\ & \left. - \frac{m_{jM}(E_{\ell_j}) \sigma_M(E_{\ell_j}) P_M(E_0)}{P_M(E_{\ell_j})} \right] / [\sigma_M(E_0) - \sigma_j(E_0)] x \end{aligned} \quad (9)$$

where the energy spanned by these secondary ions is given by the "lower limit"

$$E_{\ell_j} = R_j^{-1} \left\{ \frac{v_M}{v_j} [R_M(E_0) - x] \right\} \quad (10)$$

and "upper limit"

$$E_{u_j} = R_j^{-1} \left[\frac{v_M}{v_j} R_M(E_0) - x \right] \quad (11)$$

The range scale parameter for the type-j ion is (ref. 3)

$$v_j = z_j^2 / A_j \quad (12)$$

The second perturbation, which yields the dose contribution from the tertiary ions, is

$$D^{(2)}(x) \approx \sum_{jk} m_{jk} \sigma_k m_{kM} \sigma_M \frac{A_j v_j (E'_{u_j} - E'_{l_j})}{(v_M - v_k)(\sigma_M - \sigma_k)x} \left[\frac{e^{-\sigma_j x} - e^{-\sigma_M x}}{\sigma_M - \sigma_j} - \frac{e^{-\sigma_j x} - e^{-\sigma_k x}}{\sigma_k - \sigma_j} \right] \quad (13)$$

where the energy range spanned by these tertiary ions is given by the upper limit

$$E'_{u_j} = R_j^{-1} \left[\frac{v_M}{v_j} R_M(E_0) - x \right] \quad (14)$$

and the corresponding lower limit

$$E'_{l_j} = R_j^{-1} \left\{ \frac{v_M}{v_j} [R_M(E_0) - x] \right\} \quad (15)$$

The parameters m and σ of equation (13) are evaluated at E_0 . The results of equations (14) and (15) are understood to be zero whenever the right-hand sides are negative. The above expressions can be applied to various shield materials of uniform composition. Each specific application requires knowledge of the appropriate transport coefficients $S_j(E)$, σ_j , and m_{jk} .

TRANSPORT COEFFICIENTS

Stopping Power

The total stopping power is obtained by adding the electronic and nuclear contributions according to the detailed methods given in reference 3. The results for various ions in polyethylene, as a function of energy, are shown in figure 1. Figure 2 shows the comparable results for Kapton.

Nuclear-Absorption Cross Section

The macroscopic nuclear-absorption cross section $\sigma_j(E)$ is determined from the expression

$$\sigma_j(E) = \sum_i \rho_i \sigma_{ij}(E) \quad (16)$$

where the values of ρ_i are the elemental constituent number densities for the absorber, and the values of $\sigma_{ij}(E)$ are the "microscopic" nuclear-absorption cross sections. Values of ρ_i are listed in table 1. The values of σ_{ij} were taken from references 1 and 2. Table 2 is a listing of the resultant macroscopic cross sections σ_j for various projectile ions, as a function of incident energy, in Kapton. The results for polyethylene are shown table 3. The average extinction coefficients for several projectiles are shown in table 4 for Kapton and table 5 for polyethylene. Values for intermediate energies and mass numbers can be found by numerical interpolation.

Nuclear Fragmentation Parameters

The basic fragmentation parameters, or multiplicities, for projectile nuclei colliding with an absorber are determined from the expression

$$m_{jk}(E) = \frac{\sigma(Z_k, A_k, A_T, Z_j, A_j, E)}{\sigma_k(A_T, E)} \quad (17)$$

where $\sigma(Z_k, A_k, A_T, Z_j, A_j, E)$ is the partial production cross section for a fragment of type A_j and Z_j produced by an ion of type A_k and Z_k colliding with a target of mass A_T , and where $\sigma_k(A_T, E)$ is the macroscopic absorption cross section for the k th incident ion colliding with the target of mass number A_T . The partial production cross sections are those obtained from the semiempirical formulas of Silberberg and Tsao (ref. 4) augmented by the light fragment production cross sections of Bertini (ref. 5). These have been modified, however, in two ways: (1) Rather than scaling by total ion kinetic energy, as suggested in reference 4, the relative target velocity (energy per nucleon) was assumed to be the appropriate parameter for evaluating the hydrogen fragmentation cross sections, since particle velocity, rather than total kinetic energy, is approximately conserved in these interactions (refs. 6 and 7); and (2) To account for the lack of fragment mass and charge conservation in reference 4, the fragmentation parameters are renormalized to ensure mass and charge conservation. The multiplicative renormalization factor is

$$F = \left[(Z_p A_p) / (Z_S A_S) \right]^{1/2} \quad (18)$$

where Z_S and A_S are the total fragment charge and mass obtained from the formulation of reference 4, and Z_p and A_p are the incident projectile ion charge and mass. Fragmentation parameters and total renormalized fragment charge for ^{20}Ne beams onto Kapton and polyethylene are given in tables 6 and 7 for a broad range of energies.

^{20}Ne DEPTH-DOSE RELATIONS

The relative doses as a function of depth for ^{20}Ne beams at 350, 670, and 2000 MeV/amu, obtained from equations (5), (9), and (13), are displayed in figures 3 through 5 for a Kapton absorber, and in figures 6 through 8 for a polyethylene absorber. The curves at 350 and 670 MeV/amu show that the dose from secondary and tertiary ions is substantial (nearly 50 percent of the entering dose) for several centimeters beyond the depths where the primary beam is completely attenuated (in the region of the Bragg peak). At 2000 MeV/amu no Bragg peak is visible. The large production of secondaries and tertiaries, however, yields substantial doses even though the primary beam is largely attenuated. For a Kapton absorber, for example, figure 5 indicates that 30 cm of absorber reduces the dose from the primary beam to about 10 percent of its initial value at the absorber surface. The production of secondaries and tertiaries due to nuclear fragmentations, however, increases the total dose to over 25 percent of its initial value. It is not until an absorber depth of about 50 cm is reached that the total dose is reduced to 10 percent of its initial value. At this depth the primary beam dose is only 2 percent of its initial value. Comparable results are seen in figure 8 for polyethylene. A relative comparison of the effectiveness of Kapton and polyethylene as a shield material is not included in this report, because these predicted depth-dose values have not yet been validated by experiment. In addition, a more meaningful comparison needs to consider the isotopic composition of the total beam, since different nuclear species produced by the fragmentations could have drastically different biological effects on astronauts because of the differing RBE's (relative biological efficiency) of the various nuclear species. Finally, the theory does not yet include contributions from higher-order terms (above tertiary), which may be significant at greater absorber depths.

CONCLUDING REMARKS

Transport coefficients for heavy-ion transport in polyethylene and Du Pont Kapton have been calculated and utilized in an energy-dependent theory to predict depth-dose results for galactic, cosmic-ray, neon nuclei impinging upon a homogeneous shield composed of these organic composite materials. The importance of secondary and subsequent-generation ions produced by the nuclear fragmentation of the incident particles within the absorber was clearly demonstrated.

Langley Research Center
National Aeronautics and Space Administration
Hampton, VA 23665
December 12, 1983

REFERENCES

1. Townsend, Lawrence W.; Wilson, John W.; and Bidasaria, Hari B.: Heavy-Ion Total and Absorption Cross Sections Above 25 MeV/Nucleon. NASA TP-2138, 1983.
2. Townsend, Lawrence W.; Wilson, John W.; and Bidasaria, Hari B.: Nucleon and Deuteron Scattering Cross Sections From 25 MeV/Nucleon to 22.5 GeV/Nucleon. NASA TM-84636, 1983.
3. Wilson, John W.: Heavy Ion Transport in the Straight Ahead Approximation. NASA TP-2178, 1983.
4. Silberberg, R.; Tsao, C. H.; and Shapiro, M. M.: Semiempirical Cross Sections, and Applications to Nuclear Interactions of Cosmic Rays. Spallation Nuclear Reactions and Their Applications, B. S. P. Shen and M. Merker, eds., D. Reidel Pub. Co., c.1976, pp. 49-81.
5. MECC-7 Intranuclear Cascade Code, 500-MeV Protons on O-16. I4C Analysis Codes (Programmed for H. W. Bertini). Available from Radiation Shielding Information Center, Oak Ridge National Laboratory, 1968.
6. Schimmerling, Walter; Curtis, Stanley B.; and Vosburgh, Kirby G.: Velocity Spectrometry of 3.5-GeV Nitrogen Ions. Radiat. Res., vol. 72, no. 1, Oct. 1977, pp. 1-17.
7. Townsend, L. W.; and Deutchman, P. A.: Isobar Giant Resonance Formation in Self-Conjugate Nuclei. Nucl. Phys. A, vol. 355, 1981, pp. 505-532.

SYMBOLS

A_j	atomic mass of type-j ion, amu
A_T	mass number, dimensionless
$D(x)$	energy absorbed per unit mass at x , MeV/g
E	ion kinetic energy, MeV/amu
E_x	residual energy, MeV/amu
E_0	incident beam energy, MeV/amu
j	type-j ion
k	type-k ion
$m_{jk}(E)$	multiplicity of type-j ions produced by collisions of type-k ions of energy E
$O_M(E)$	average extinction coefficient for type-M ions, cm^{-1}
$P_M(E)$	nuclear attenuation factor for type-M ion at energy E , dimensionless
$R_j(E)$	continuous slowing-down range of type-j ion of energy E , cm
$R_j^{-1}[R_j(E)]$	inverse function of $R_j(E)$
$S_j(E)$	total stopping power or linear energy transfer (LET) due to interaction of type-j ion with orbital electrons of transport medium, MeV/cm
$\tilde{S}_j(E)$	stopping power or linear energy transfer (LET) per nucleon due to interaction of type-j ion with orbital electrons of transport medium, MeV/amu-cm
x	one-dimensional position vector, g/cm^2
Z_j	atomic number of type-j ion
v_j	range scale parameter for type-j ion
ρ_i	number density of i th constituent of absorber, cm^{-3}
$\sigma_j(E)$	macroscopic absorption cross section for type-j ion of energy E , cm^{-1}
$\sigma_{ij}(E)$	microscopic absorption cross section for type-j particle of energy E colliding with type-i particle in absorber, cm^2
$\Phi_j(x, E)$	differential flux of type-j ions at x with energy E , $(\text{cm}^2\text{-sec-MeV/amu})^{-1}$

Subscripts:

M type of ions in monoenergetic beam

P projectile

S Silberberg-Tsao formalism

Superscripts:

(0),(1),(2) terms in series approximation to equation (3)

Primes indicate a variable of summation or integration.

TABLE 1.- CONSTITUENT NUMBER DENSITIES FOR KAPTON
AND POLYETHYLENE

Constituent	Number density, ρ_i , 10^{22} atoms/cm ³ , for -	
	Kapton (1.42 g/cm ³)	Polyethylene (0.91 g/cm ³)
Hydrogen	2.239	7.826
Carbon	4.925	3.913
Nitrogen	.448	
Oxygen	1.119	

TABLE 2.- MACROSCOPIC NUCLEAR-ABSORPTION CROSS SECTIONS IN KAPTON

E, MeV/amu	Macroscopic nuclear-absorption cross section, $\sigma_j(E)$, 10^{-4} /cm, in Kapton for -										
	¹ H	⁴ He	⁷ Li	⁹ Be	¹² C	¹⁶ O	²⁰ Ne	²⁷ Al	⁴⁰ Ar	⁵⁶ Fe	⁶⁴ Cu
25	323	526	789	862	861	1012	1084	1118	1455	1630	1690
50	249	430	645	713	727	858	924	971	1260	1430	1490
75	215	387	582	648	667	790	853	905	1175	1340	1400
100	191	355	534	597	621	738	799	855	1109	1273	1334
200	158	308	466	526	556	663	722	782	1016	1176	1237
300	149	296	447	506	538	643	701	762	990	1150	1210
400	152	300	452	511	543	648	707	767	997	1156	1217
600	175	328	492	554	583	694	754	813	1052	1215	1276
1000	189	346	517	581	609	723	784	842	1089	1253	1314
2000	191	353	525	589	618	732	794	852	1100	1266	1330
4000	188	350	520	584	614	728	789	848	1095	1260	1322
10000	185	347	515	578	609	722	783	843	1088	1250	1315

TABLE 3.- MACROSCOPIC NUCLEAR-ABSORPTION CROSS SECTIONS IN POLYETHYLENE

$$[\rho = 0.91 \text{ g/cm}^3]$$

E, MeV/amu	Macroscopic nuclear-absorption cross section, $\sigma_j(E)$, $10^{-4}/\text{cm}$, in polyethylene for -										
	^1H	^4He	^7Li	^9Be	^{12}C	^{16}O	^{20}Ne	^{27}Al	^{40}Ar	^{56}Fe	^{64}Cu
25	256	428	717	795	786	951	1038	1078	1471	1667	1733
50	179	342	564	635	648	787	861	919	1242	1433	1500
75	145	304	499	565	585	713	783	848	1143	1330	1402
100	127	275	448	511	536	655	723	792	1067	1250	1323
200	105	235	376	435	468	572	636	710	956	1134	1206
300	100	224	357	414	448	550	613	686	922	1100	1172
400	104	227	361	418	454	556	619	692	930	1110	1180
600	125	252	400	460	496	606	671	743	994	1177	1248
1000	139	268	425	488	523	638	705	775	1036	1220	1292
2000	138	274	433	497	531	646	715	786	1050	1236	1308
4000	134	272	427	490	527	641	708	781	1041	1228	1300
10000	132	270	421	484	522	634	702	774	1032	1220	1290

TABLE 4.- AVERAGE EXTINCTION COEFFICIENTS FOR IONS IN KAPTON

E, MeV/amu	Average extinction coefficient, O_k , $10^{-4}/\text{cm}$, in Kapton for -										
	^1H	^4He	^7Li	^9Be	^{12}C	^{16}O	^{20}Ne	^{30}Si	^{40}Ar	^{50}V	^{60}Ni
25	323	526	789	862	860	1011	1083	1167	1452	1572	1659
50	290	483	725	795	801	944	1013	1102	1371	1490	1579
75	259	443	665	734	746	880	947	1040	1291	1409	1497
100	236	414	622	689	704	833	898	993	1232	1347	1435
200	189	351	528	591	615	731	793	892	1103	1213	1300
300	171	325	491	552	580	691	750	851	1051	1160	1246
400	163	315	475	535	565	673	733	833	1029	1137	1222
600	163	314	473	534	564	672	731	832	1026	1134	1220
1000	174	327	492	553	582	693	753	854	1052	1161	1247
2000	184	342	510	574	602	715	776	877	1079	1189	1276
4000	187	347	517	581	610	724	785	886	1090	1200	1287
10000	187	348	517	581	611	724	785	887	1091	1200	1287

TABLE 5.- AVERAGE EXTINCTION COEFFICIENTS FOR IONS IN POLYETHYLENE

$$[\rho = 0.91 \text{ g/cm}^3]$$

E, MeV/amu	Average extinction coefficient, O_K , $10^{-4}/\text{cm}$, in polyethylene for -										
	^1H	^4He	^7Li	^9Be	^{12}C	^{16}O	^{20}Ne	^{30}Si	^{40}Ar	^{50}V	^{60}Ni
25	256	428	717	795	786	950	1037	1135	1468	1603	1700
50	221	389	648	723	725	878	959	1064	1372	1506	1605
75	189	354	586	657	667	810	886	996	1279	1410	1511
100	167	328	540	609	623	759	832	945	1209	1338	1439
200	128	272	442	504	530	647	715	832	1058	1180	1281
300	115	250	403	463	492	602	668	786	996	1116	1215
400	110	240	386	445	476	583	648	765	969	1088	1187
600	112	240	383	442	476	582	646	764	965	1085	1183
1000	123	252	400	461	495	605	671	788	994	1115	1214
2000	133	264	419	481	516	629	696	813	1026	1148	1247
4000	135	269	425	488	523	637	705	823	1037	1160	1260
10000	133	270	424	487	524	637	704	824	1036	1160	1260

TABLE 6.- ^{20}Ne FRAGMENTATION PARAMETERS IN KAPTON AND
TOTAL FRAGMENT CHARGE Z_F

Z_F	^{20}Ne fragmentation parameters in Kapton for E, MeV/amu, of -					
	10	31.6	100	316	1000	3160
0	1.312	0.968	0.961	1.287	2.158	3.420
1	3.139	2.170	1.974	2.375	3.177	3.812
2	.971	.713	.587	.524	.651	.600
3	.036	.024	.032	.047	.083	.095
4	.043	.028	.037	.051	.080	.087
5	.003	.013	.035	.061	.074	.073
6	.005	.026	.080	.121	.111	.100
7	.020	.048	.090	.106	.083	.073
8	.193	.225	.289	.267	.183	.158
9	.302	.268	.217	.195	.158	.121
10	.008	.159	.122	.077	.060	.053
11	.043	.009	.002	.000	.000	.000
\bar{Z}_F	10.4	10.2	10.2	10.2	10.2	10.0

TABLE 7.- ^{20}Ne FRAGMENTATION PARAMETERS IN POLYETHYLENE AND TOTAL
FRAGMENT CHARGE \bar{Z}_F

Z_F	^{20}Ne fragmentation parameters in polyethylene for E , MeV/amu, of -					
	10	31.6	100	316	1000	3160
0	1.313	0.968	0.962	1.288	2.162	3.427
1	3.141	2.171	1.975	2.378	3.182	3.819
2	.971	.713	.588	.525	.653	.601
3	.035	.023	.031	.046	.081	.093
4	.042	.026	.036	.050	.078	.086
5	.003	.013	.035	.060	.074	.072
6	.005	.026	.080	.121	.111	.100
7	.020	.048	.090	.106	.083	.073
8	.193	.225	.289	.267	.183	.159
9	.303	.268	.217	.195	.158	.121
10	.008	.159	.122	.077	.060	.053
11	.043	.009	.002	.000	.000	.000
\bar{Z}_F	10.4	10.2	10.2	10.2	10.2	10.0

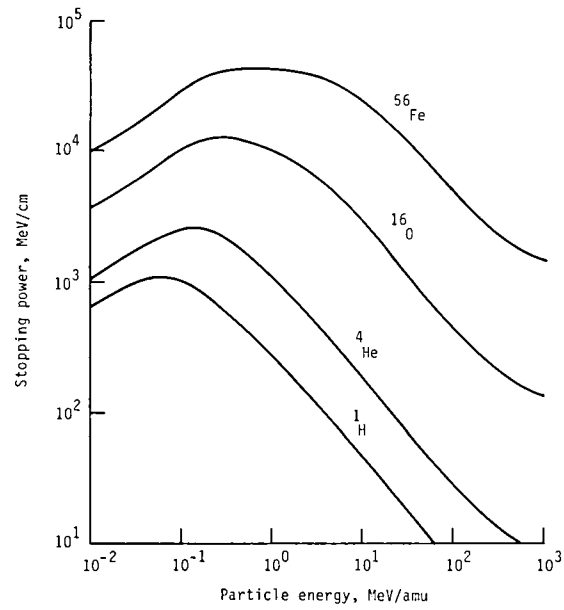


Figure 1.- Calculated stopping powers in polyethylene for typical cosmic-ray ions as a function of kinetic energy.

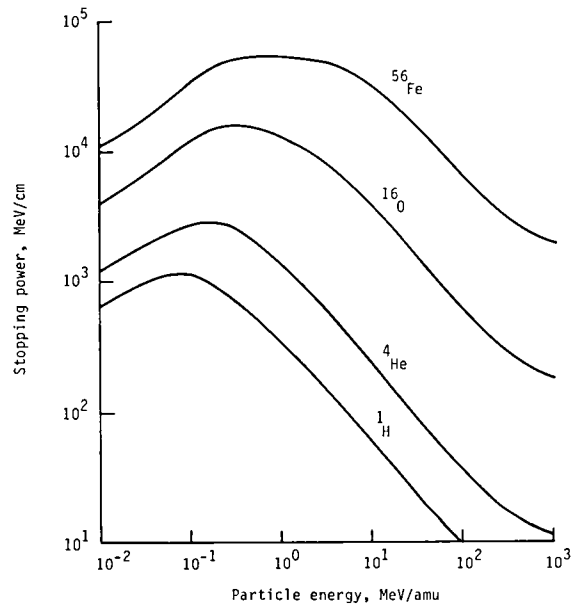


Figure 2.- Calculated stopping powers in Kapton for typical cosmic-ray ions as a function of kinetic energy.

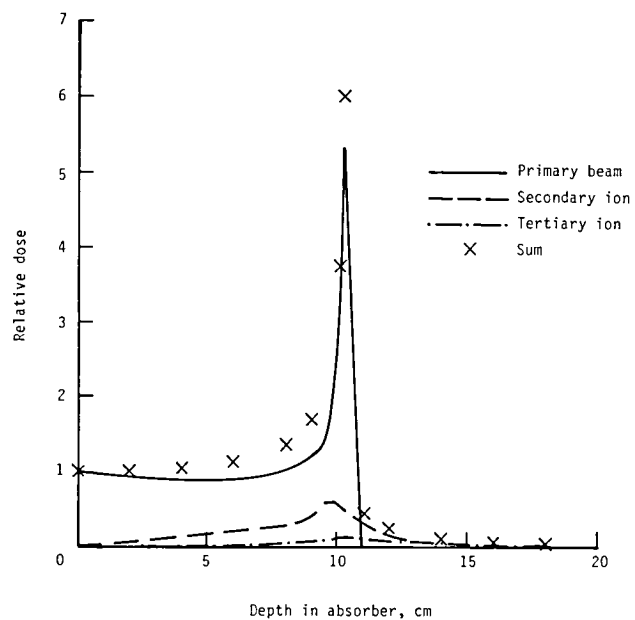


Figure 3.- Relative dose as a function of depth in absorber for 350-MeV/amu ^{20}Ne incident on Kapton.

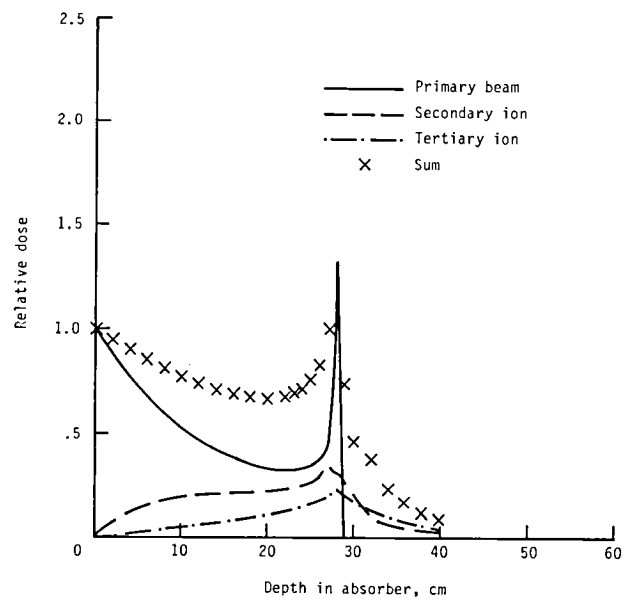


Figure 4.- Relative dose as a function of depth in absorber for 670-MeV/amu ^{20}Ne incident on Kapton.

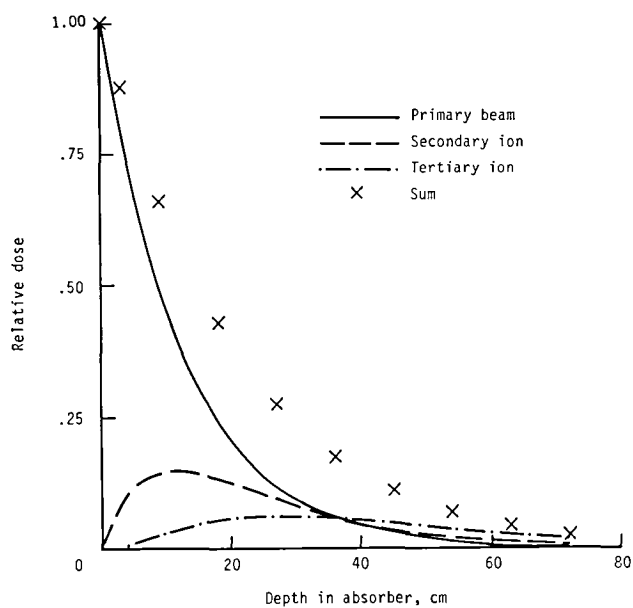


Figure 5.- Relative dose as a function of depth in absorber for 2000-MeV/amu ^{20}Ne incident on Kapton.

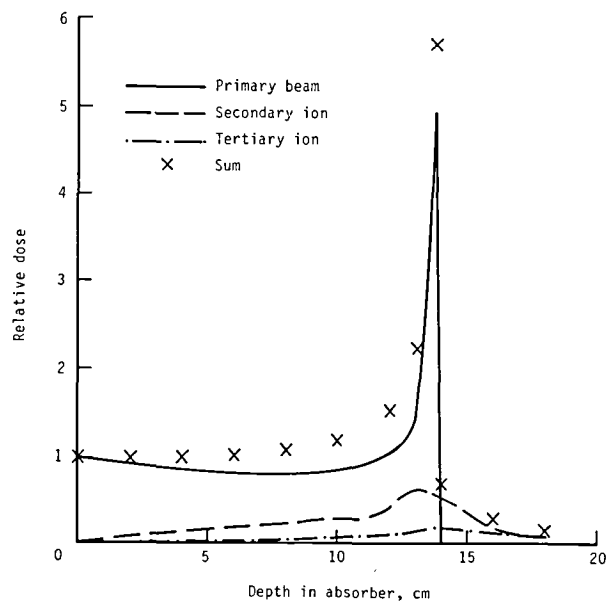


Figure 6.- Relative dose as a function of depth in absorber for 350-MeV/amu ^{20}Ne incident on polyethylene.

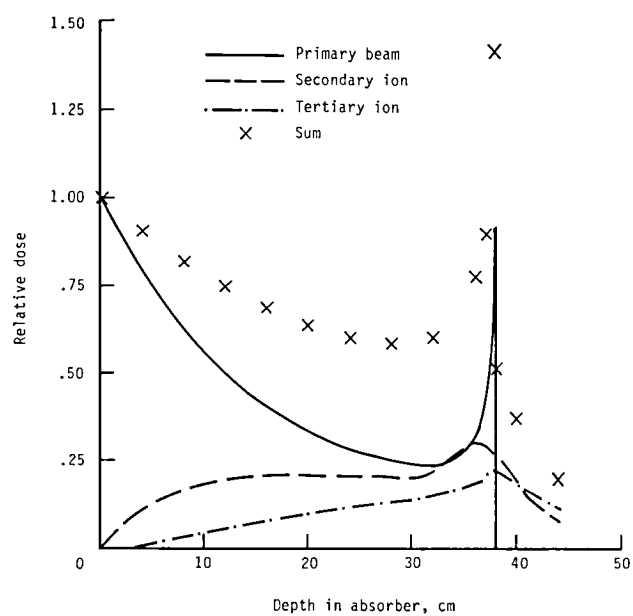


Figure 7.- Relative dose as a function of depth in absorber for 670-MeV/amu ^{20}Ne incident on polyethylene.

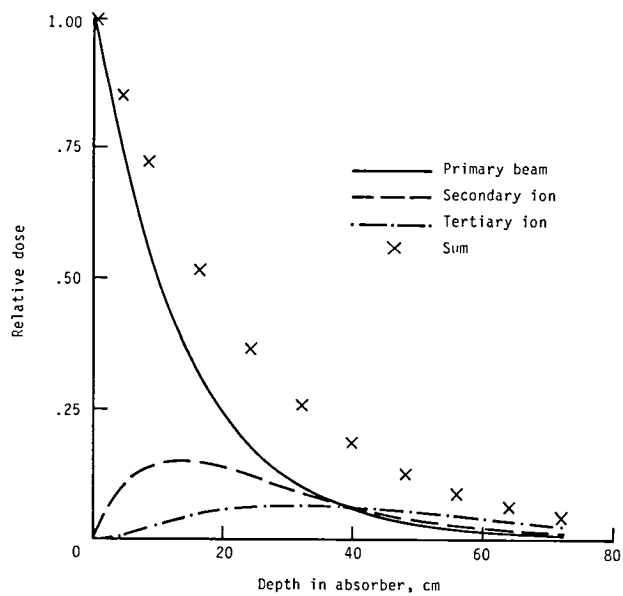


Figure 8.- Relative dose as a function of depth in absorber for 2000-MeV/amu ^{20}Ne incident on polyethylene.

1. Report No. NASA TM-85693		2. Government Accession No.		3. Recipient's Catalog No.	
4. Title and Subtitle NEON TRANSPORT IN SELECTED ORGANIC COMPOSITES				5. Report Date February 1984	
				6. Performing Organization Code 199-20-76-01	
7. Author(s) Lawrence W. Townsend, John W. Wilson, and Hari B. Bidasaria				8. Performing Organization Report No. L-15690	
				10. Work Unit No.	
9. Performing Organization Name and Address NASA Langley Research Center Hampton, VA 23665				11. Contract or Grant No.	
				13. Type of Report and Period Covered Technical Memorandum	
12. Sponsoring Agency Name and Address National Aeronautics and Space Administration Washington, DC 20546				14. Sponsoring Agency Code	
15. Supplementary Notes Lawrence W. Townsend and John W. Wilson: Langley Research Center, Hampton, Virginia. Hari B. Bidasaria: Old Dominion University, Norfolk, Virginia.					
16. Abstract Utilizing an energy-dependent, perturbation expansion solution for heavy-ion transport in one dimension, the dose has been calculated from ^{20}Ne beams, at incident kinetic energies of 350, 670, and 2000 MeV/amu onto selected organic composites. Transport coefficients, applicable to arbitrary ion beams over a broad range of energies, are also presented.					
17. Key Words (Suggested by Author(s)) Heavy-ion transport Organic composites Shielding			18. Distribution Statement Unclassified - Unlimited Subject Category 73		
19. Security Classif. (of this report) Unclassified	20. Security Classif. (of this page) Unclassified	21. No. of Pages 18	22. Price A02		

National Aeronautics and
Space Administration

Washington, D.C.
20546

Official Business

Penalty for Private Use, \$300

THIRD-CLASS BULK RATE

Postage and Fees Paid
National Aeronautics and
Space Administration
NASA-451



NASA

POSTMASTER:

If Undeliverable (Section 158
Postal Manual) Do Not Return
